HHS Public Access

Author manuscript

*JACC Clin Electrophysiol*. Author manuscript; available in PMC 2018 February 23.

Published in final edited form as:

*JACC Clin Electrophysiol*. 2018 January ; 4(1): 17–29. doi:10.1016/j.jacep.2017.07.019.

# Relationship Between Fibrosis Detected on Late Gadolinium-Enhanced Cardiac Magnetic Resonance and Re-Entrant Activity Assessed With Electrocardiographic Imaging in Human Persistent Atrial Fibrillation

**Hubert Cochet, MD, PhD**[a,b], **Rémi Dubois, PhD**[b], **Seigo Yamashita, MD**[a], **Nora Al Jefairi, MD**[a], **Benjamin Berte, MD**[a], **Jean-Marc Sellal, MD**[a], **Darren Hooks, MD**[a], **Antonio Frontera, MD**[a], **Sana Amraoui, MD**[a,b], **Adlane Zemoura, MD**[a,b], **Arnaud Denis, MD**[a,b], **Nicolas Derval, MD**[a,b], **Frederic Sacher, MD, PhD**[a,b], **Olivier Corneloup, MD**[a], **Valérie Latrabe, MD**[a], **Stéphanie Clément-Guinaudeau, MD**[a], **Jatin Relan, PhD**[c], **Sohail Zahid, PhD**[d], **Patrick M. Boyle, PhD**[d], **Natalia A. Trayanova, PhD**[d], **Olivier Bernus, PhD**[b], **Michel Montaudon, MD, PhD**[a,b], **François Laurent, MD**[a,b], **Mélèze Hocini, MD**[a,b], **Michel Haïssaguerre, MD**[a,b], and **Pierre Jaïs, MD**[a,b]

[a]Haut-Lévêque Cardiology Hospital, Bordeaux University Hospital Center, University of Bordeaux, France [b]National Institute for Health and Medical Research (INSERM) U1045 – Electrophysiology and Heart Modeling Institute, Bordeaux, France [c]St. Jude Medical, St. Paul, Minnesota [d]Institute for Computational Medicine, Department of Biomedical Engineering, Johns Hopkins University, Baltimore, Maryland

## Abstract

**OBJECTIVES—**This study sought to assess the relationship between fibrosis and re-entrant activity in persistent atrial fibrillation (AF).

**BACKGROUND—**The mechanisms involved in sustaining re-entrant activity during AF are poorly understood.

**METHODS—**Forty-one patients with persistent AF (age 56 ± 12 years; 6 women) were evaluated. High-resolution electrocardiographic imaging (ECGI) was performed during AF by using a 252-chest electrode array, and phase mapping was applied to locate re-entrant activity. Sites of high re-entrant activity were defined as re-entrant regions. Late gadolinium-enhanced (LGE) cardiac magnetic resonance (CMR) was performed at 1.25 × 1.25 × 2.5 mm resolution to characterize atrial fibrosis and measure atrial volumes. The relationship between LGE burden and the number of re-entrant regions was analyzed. Local LGE density was computed and characterized at re-entrant sites. All patients underwent catheter ablation targeting re-entrant regions, the procedural endpoint being AF termination. Clinical, CMR, and ECGI predictors of acute procedural success were then analyzed.

ADDRESS FOR CORRESPONDENCE: Dr. Hubert Cochet, Unité d'Imagerie Thoracique et Cardiovasculaire, Hôpital Cardiologique du Haut-Lévêque, Avenue de Magellan, 33604 Bordeaux-Pessac, France. hcochet@wanadoo.fr.

**RESULTS—**Left atrial (LA) LGE burden was 22.1 ± 5.9% of the wall, and LA volume was 74 ± 21 ml/$m^2$. The number of re-entrant regions was 4.3 ± 1.7 per patient. LA LGE imaging was significantly associated with the number of re-entrant regions (R = 0.52, p = 0.001), LA volume (R = 0.62, p < 0.0001), and AF duration (R = 0.54, p = 0.0007). Regional analysis demonstrated a clustering of re-entrant activity at LGE borders. Areas with high re-entrant activity showed higher local LGE density as compared with the remaining atrial areas (p < 0.0001). Failure to achieve AF termination during ablation was associated with higher LA LGE burden (p < 0.001), higher number of re-entrant regions (p < 0.001), and longer AF duration (p = 0.008).

**CONCLUSIONS—**The number of re-entrant regions during AF relates to the extent of LGE on CMR, with the location of these regions clustering to LGE areas. These characteristics affect procedural outcomes of ablation.

### Keywords

atrial fibrillation; atrial fibrosis; electrocardiographic mapping; magnetic resonance imaging; re-entry; rotor

Atrial fibrillation (AF) is a major cause of heart failure and stroke (1). In its persistent form, the arrhythmia is thought to be triggered by focal sources of automatic discharge and maintained by reentrant activities organizing within the atrial tissue, the so-called rotors, sustaining high-frequency activity (2–4). Noninvasive electrocardiographic imaging (ECGI) mapping has been introduced for real-time and whole-heart mapping of cardiac electrical activity (5). The technique was validated versus high-density contact mapping in animals (6,7), and it has been applied in humans to study ventricular (8) and atrial arrhythmias (9,10), as well as conduction disturbances in heart failure (11). In patients with persistent AF, regions harboring re-entrant activity can be identified by phase map calculation from either contact data acquired with biatrial basket catheters (12) or noncontact data acquired by ECGI (9). Using these methods, clinical reports have demonstrated the benefit of a tailored ablation approach targeting patient-specific re-entrant drivers (12,13). Conversely, interstitial fibrosis is consistently present in patients with AF (14,15). Experimental data have shown that re-entry can be induced and maintained by both electrophysiological and structural remodeling and that fibrosis plays a major role in the mechanisms of fibrillation organization (16–19). However, the latter relationship has not been thoroughly studied in humans. Developments in cardiac magnetic resonance (CMR) techniques now enable the acquisition of late gadolinium-enhanced (LGE) images with sufficient spatial resolution to study the atrial wall (20). Because gadolinium-based contrast agents have an interstitial distribution, areas of LGE in the atrium represent areas where interstitial fibrosis is the most pronounced, as reported by histological studies (21). The aim of this study was to analyze the relationship between LGE as assessed on CMR and re-entrant activity as identified by ECGI in persistent AF.

## METHODS

### POPULATION

From June 2013 to October 2014, 41 patients (age 56 ± 12 years; 6 women) were included in the study. Inclusion criteria were as follows: the presence of persistent AF, defined as

uninterrupted AF lasting longer than 7 days; and an indication for catheter ablation according to current guidelines (22). Exclusion criteria were contraindications to CMR, a history of prior cardiac ablation or atrial surgery, and the presence of intracardiac thrombus on trans-esophageal echocardiography. These 41 patients were not consecutive because the inclusion was also dependent on the availability of CMR. All patients underwent routine medical history, physical examination, and laboratory assessment of renal function. Persistent AF duration was calculated from the time of initial diagnosis in the absence of intercurrent documentation of sinus rhythm. Long-standing persistent AF was defined as uninterrupted AF lasting more than 12 months. The study was approved by the local Institutional Ethics Committee, and all patients gave informed consent.

## CARDIAC MAGNETIC RESONANCE

Imaging was performed 1 to 3 days before ECGI and catheter ablation on a 1.5-T device (Magnetom Avanto, Siemens Medical Systems, Erlangen, Germany) equipped with a 32-channel coil dedicated to cardiac imaging. Cine imaging was performed using a breath-held, electrocardiographically gated steady-state free precession pulse sequence to acquire a stack of 4-chamber slices covering both atria from roof to bottom (slice thickness, 6 mm; temporal resolution, 15 ms). Atrial LGE acquisition was initiated 15 min after the intravenous injection of 0.2 mmol/kg gadoterate meglumine (Guerbet, Aulnay-sous-bois, France). Imaging was performed using a 3-dimensional, inversion-recovery-prepared, electrocardiographically gated, respiration-navigated gradient-echo pulse sequence with fat saturation (20). Typical imaging parameters were as follows: voxel size 1.25 × 1.25 × 2.5 mm; flip angle 22°; repetition time (TR)/echo time (TE) 6.1/2.4 ms; inversion time 260 to 320 ms, depending on the results of a TI scout scan performed immediately before acquisition; parallel imaging with GRAPPA technique (Siemens Healthineers, Erlangen, Germany) with R = 2; 42 reference lines; and acquisition time 5 to 10 min, depending on patient's heart and breath rate.

## IMAGE PROCESSING

On cine images, the left atrial (LA) endocardium was manually segmented using Argus software (Siemens Medical Solutions, Erlangen, Germany) to compute LA maximal volume, expressed in $ml/m^2$. The assessment of LGE image quality is detailed in the Online Appendix. Briefly, image quality was analyzed by 2 observers to select the datasets eligible for global LGE quantification (excluding datasets of poor quality) and for regional LGE characterization (performed only on datasets of excellent quality). In patients eligible for global LGE quantification, the wall of both the left and right atria was manually traced, and significant LGE was segmented by adaptive thresholding of myocardial voxels as described previously (20), by using Music software (MUSIC software, Electrophysiology and Heart Modeling Institute, University of Bordeaux, Bordeaux, France; and Inria, Sophia Antipolis, France). The output of the segmentation was a global quantification of LGE burden, expressed in percentage of the wall in the left atrium, right atrium, and both atria. LGE burden within the left atrium was categorized according to the Utah method: class I, 0% to 10%; class II, 10% to 20%; class III, 20% to 30%; and class IV, more than 30% (23). The reproducibility of LGE quantification is analyzed in the Online Appendix. In the subset of patients eligible for regional analysis, LGE segmentation was used to compute a patient-

specific 3-dimensional map of LGE over the biatrial geometry, as implemented in VTK (Visualization Toolkit, Kitware, Inc., New York, New York). In addition, LGE segmentations were used to compute a finite element mesh at high density (increased spatial resolution being implemented for visualization purposes) (Online Figure 1). From this mesh, regional LGE patterns were characterized by computing local LGE density (local burden, expressed as a percentage) over a 5-mm kernel, and this metric was mapped over the biatrial geometry. Details on the computation of this LGE descriptor, as implemented in MATLAB software (Mathworks, Natick, Massachusetts), are provided in the Online Appendix. Briefly, at each point of the mesh local LGE density refers to the percentage of neighboring points exhibiting LGE; this means that local LGE density is expected to be close to 0 outside LGE, close to 1 inside LGE, and approximately 0.5 on LGE borders. The image processing strategy is illustrated in Figures 1A to 1D.

## ELECTROCARDIOGRAPHIC MAPPING AND PROCESSING

ECGI was performed at the bedside within 24 h preceding the ablation procedure in patients presenting with AF. In patients presenting in sinus rhythm, AF was induced in the laboratory by rapid atrial pacing before transseptal puncture, and ECGI was performed after 30 min of sustained AF. The acquisition was performed using a commercially available system (CardioInsight Technologies, Inc., Cleveland, Ohio). A 252-electrode vest was positioned on the patient's thorax and abdomen to record body surface potentials. The localization of each electrode with respect to the biatrial epicardium was achieved immediately before mapping by using a 64-element computed tomography scanner (Somatom Definition, Siemens Medical Systems, Forchheim, Germany). Imaging was performed without contrast media injection or cardiac synchronization, thus resulting in a radiation exposure lower than 2 mSv in all cases. The segmentation and labeling of each electrode were performed automatically. The segmentation of the atrial epicardium was performed manually. ECGI aimed at acquiring 10 to 15 s of AF, separated in cardiac pauses to exclude QRS complexes and T waves from mapping windows. The reconstruction of unipolar electrograms from body surface potentials was performed using a dedicated algorithm, as described previously (6). From unipolar electrograms, local phase was computed to visualize electrical activation during AF, and automatic detection of phase singularities was implemented to detect re-entrant activity (9). A reentry was defined as any phase singularity lasting more than 200 ms (at least 2 rotations). The output of signal processing was a 3-dimensional map of phase singularities' trajectories over a biatrial surface and a biatrial map displaying re-entry statistics. On each point of the geometry, this refers to the probability of observing a re-entry at a given time frame. Regions of high re-entrant activity were defined as regions with a local re-entry statistic >0.002. This threshold was set so that the atrial surface described as a re-entrant region corresponded to the surface usually covered by ablation before reaching the ablation endpoint in patients with persistent AF (10% to 15% of the total biatrial surface), as detailed in the Online Appendix (Online Figure 2). These re-entrant regions were those considered to be drivers and subsequently targeted by ablation. For each patient, the number of regions was assessed on cumulative maps of rotor statistics, and the spatial separation between 2 regions used the threshold applied on this statistic as its basis. The processing of ECGI data is illustrated in Figures 2A to 2D.

## REGISTRATION BETWEEN CMR AND ECGI

CMR biatrial maps displaying LGE and local LGE density were registered to the ECGI geometry. Registration was performed using landmark-based registration with affine anisotropic transformation, as implemented in VTK (Kitware, Inc., New York, New York). The transform was defined by 2 sets of 12 landmarks placed on each geometry: 1 at the tip of each of the 4 pulmonary veins, 1 on each vena cava, 1 at the tip of each appendage, and 1 on anterior and posterior aspects of the left and right atria. The computed transform gives the best fitted map in a least square sense and with collinearity preserved. Details of the algorithm have been previously described (24,25). The root mean square error on distance after registration was 3.0 ± 1.2 mm. Once registered, the LGE descriptors were projected along the surface normal direction onto the ECGI geometry. To minimize interpolation errors during projection, both the CMR and ECGI meshes were generated with high spatial resolution (more than $10^5$ triangles). In addition to the direct correlation between re-entrant activity and local LGE density at all points of the geometry, we also analyzed the agreement between re-entrant regions and LGE distributions by using a biatrial 7-segment model as described in Haïssaguerre et al. (13) In all 20 patients eligible for regional analysis, each segment was categorized as LGE+or LGE−, and Re-entry+or Re-entry−. All segments exhibiting LGE were categorized as LGE+, whereas re-entrant regions were attributed to the segment covering most of their surface.

## CATHETER ABLATION PROCEDURE

Transesophageal echocardiography was performed within 5 days before the procedure. The ablation of re-entrant regions was conducted as previously described by Haïssaguerre et al. (13). Briefly, the atria were accessed through a right femoral vein and a transseptal approach. A steerable decapolar catheter (Xtrem, Sorin Medical, Montrouge, France) was positioned in the coronary sinus, and an irrigated-tip quadripolar catheter (Thermocool, Biosense-Webster, Diamond Bar, California) was used for ablation. Ablation was performed sequentially on all regions exhibiting high re-entrant activity, as defined earlier, with regions treated in decreasing order of re-entry statistics. Radiofrequency was delivered sequentially to each region at the power of 30 to 40 W to induce point-by-point lesions covering the area of interest. The endpoint of regional ablation was local electrogram slowing and organization. The procedural endpoint was AF termination (26). If AF still persisted after the ablation of all re-entrant regions, linear lesions were added on the LA roof and mitral isthmus. When AF terminated as atrial tachycardia, ablation was pursued to eliminate 1 or more sequential circuits until sinus rhythm was restored. Pulmonary vein isolation was completed in sinus rhythm by adding more lesions to close the gap, if required, at the end of the procedure. If AF persisted after completion of the ablation protocol, cardioversion was performed. AF recurrence was assessed during follow-up on the basis of clinical interrogation and 24-hour Holter monitor recordings at 3, 6, 9, and 12 months.

## STATISTICAL ANALYSIS

The Shapiro-Wilk test of normality and D'Agostino tests for skewness and kurtosis were used to assess whether quantitative data conformed to the normal distribution. Square-root transformation was applied in case of non-normal distribution. If data were normally

distributed, parametric tests were applied on transformed data. If non-normally distributed, nonparametric tests were applied on the original data. Continuous variables are expressed as mean ±SD when of normal distribution and median [interquartile range: Q1 to Q3] otherwise. Categorical variables are expressed as fractions (%). Continuous variables were compared using independent-sample parametric (unpaired Student *t* test) or nonparametric tests (Mann-Whitney *U* test), depending on data normality. Categorical variables were compared using chi-square tests. Relationships among continuous variables were assessed using Pearson or Spearman correlation coefficients (R), depending on data normality. Stepwise hierarchical forward multiple regression analysis was performed to identify predictors of re-entrant activity, by using the criterion of $p < 0.05$ on univariable analysis for inclusion in the multivariable model. Multivariable logistic regression analyses were used to identify baseline predictors of short-term procedural success (AF termination). Assuming an expected response rate of about two-thirds on the basis of a prior publication (13), the study was populated to enable the inclusion of 2 variables in predictive models (27). Therefore, if more than 2 baseline characteristics were related to AF termination on univariable analysis, sequential regression analyses were conducted by combining characteristics by pairs. The number of measures of local LGE characteristics was too high to take into account repeated measurements within patients (between 1 and 2 million values per patient). Therefore, for practical reasons, local LGE density was described from patients' median values, illustrated using boxplots, and compared between regions of high and low re-entrant activity using paired nonparametric tests (Wilcoxon signed rank tests). The agreement between distributions of LGE and re-entrant regions was assessed using the Cohen kappa analysis and sensitivity and specificity calculations. All statistical tests were 2-tailed. A p value <0.05 was considered to indicate statistical significance. Analyses were performed using NCSS 8 (NCSS Statistical Software, Kaysville, Utah).

# RESULTS

## POPULATION CHARACTERISTICS

The characteristics of the studied population (N = 41; age 56 ± 12 years; 6 women) are shown in Table 1. Uninterrupted AF duration was 8.6 ± 6.5 months, and 8 of 41 (20%) patients presented with long-standing persistent AF. Associated structural heart disease was present in 5 of 41 (12%) patients. The heart rhythm at admission and during CMR acquisition was AF in 28 of 41 (68%) patients and sinus rhythm in 13 of 41 (32%) patients. AF was successfully induced in all 13 patients presenting in sinus rhythm. ECGI was feasible in all patients. The number of re-entrant regions identified by ECGI and targeted by ablation was 4.3 ± 1.7 per patient (range 2 to 8). Re-entrant regions covered 12.0% (7.4% to 15.3%) of the biatrial surface, and the surface of single re-entrant regions was 6.8 ± 1.9 $cm^2$. In the total population, 71% of all re-entrant regions were found in the left atrium, with the remainder in the right atrium. The measurement of atrial volume from cine CMR was feasible in all patients. LA and right atrial volumes were 74 ± 21 $ml/m^2$ and 82 ± 28 $ml/m^2$, respectively. LGE segmentation was not feasible in 4 of 41 (10%) patients because of insufficient image quality. The LGE burden was 22.1 ± 5.9% of the wall on the left atrium, 17.1 ± 7.9% on the right atrium, and 19.9 ± 6.5% on both atria. The LA LGE burden was

categorized as Utah class I in 0 of 37 (0%) patients, class II in 15 of 37 (41%) patients, class III in 18 of 37 (49%) patients, and class IV in 4 of 37 (11%) patients.

## CLINICAL CORRELATES OF ATRIAL LGE

LGE burden was related to the number of re-entrant regions, and the correlation was more pronounced when considering LA LGE only ($R = 0.52$, $p = 0.001$) than when considering right atrial LGE or overall LGE on both atria ($R = 0.21$, $p = 0.22$ and $R = 0.38$, $p = 0.03$, respectively). LA LGE also related to LA volume ($R = 0.62$, $p < 0.0001$), and to uninterrupted AF duration ($R = 0.54$, $p = 0.0007$). LA LGE burden was higher in patients with long-standing persistent AF than in other patients ($26.8 \pm 5.0\%$ vs. $20.7 \pm 5.4\%$; $p = 0.005$). It was also higher in patients presenting with AF than in those presenting in sinus rhythm ($23.6 \pm 5.5\%$ vs. $18.7 \pm 5.4\%$; $p = 0.02$). No significant relationship was found between LA LGE and age ($R = 0.14$, $p = 0.41$) or female sex ($R = -0.03$, $p = 0.86$).

## CLINICAL CORRELATES OF RE-ENTRANT ACTIVITY

Univariable and multivariable analyses for the prediction of re-entrant activity are shown in Table 2. Besides atrial LGE, the number of re-entrant regions identified by ECGI related to LA volume ($R = 0.35$, $p = 0.04$) and uninterrupted AF duration ($R = 0.45$, $p = 0.005$). More re-entrant regions were found in patients with long-standing persistent AF than in other patients ($5.6 \pm 1.3$ vs. $3.9 \pm 1.6$; $p = 0.009$). More re-entrant regions were also found in patients presenting with AF at admission than in patients presenting in sinus rhythm ($4.7 \pm 1.6$ vs. $3.4 \pm 1.5$; $p = 0.02$). The number of re-entrant regions did not relate to age ($R = -0.05$, $p = 0.78$) or female sex ($R = 0.16$, $p = 0.34$). On multivariable analysis, the extent of LA LGE independently related to the number of re-entrant regions ($R^2 = 0.32$, $p = 0.006$), whereas uninterrupted AF duration and LA volume did not ($R^2 = 0.03$, $p = 0.27$, and $R^2 = 0.0001$, $p = 0.94$, respectively).

## RELATIONSHIP BETWEEN RE-ENTRANT ACTIVITY AND LOCAL LGE CHARACTERISTICS

The subpopulation included for regional analysis was composed of 20 patients (age $52 \pm 12$ years; 3 women). The number of re-entrant regions was $3.9 \pm 1.5$ per patient, uninterrupted AF duration was $9.3 \pm 6.9$ months, LA LGE burden was $23.1 \pm 5.4\%$, and LA volume was $73 \pm 22$ ml. The rate of AF termination by catheter ablation was 65% ($n = 13$ of 20). These characteristics did not differ from those of the total population. Analysis of registered ECGI and LGE CMR data showed a clustering of phase singularity trajectories at the border of fibrotic areas, as illustrated in Figure 3. When compared with the rest of the atria, sites with high re-entrant activity showed higher values of local LGE density ($34.6 \pm 15.3\%$ vs. $13.6 \pm 7.3\%$; $p < 0.0001$), as illustrated in Figure 4. When using a 7-segment biatrial segmentation, 85 (61%) of segments were categorized as LGE+, whereas 77 (55%) were categorized Re-entry+. Significant but only fair agreement was found between LGE and reentrant region distributions ($R = 0.47$, $p < 0.01$). The presence of LGE identified segments harboring re-entrant regions with good sensitivity (82%) but limited specificity (65%).

### PREDICTORS OF AF TERMINATION BY CATHETER ABLATION

Procedural characteristics are shown in Table 1. The endpoint of AF termination was met in 28 of 41 (68%) patients. In these patients, AF terminated as sinus rhythm in 9 of 28 (32%) and as atrial tachycardia in 19 of 28 (68%) patients. Atrial tachycardia was successfully terminated by additional ablation in 19 of 19 (100%) patients. The ablation set comprised reentrant regions and additional ablation to complete pulmonary vein isolation in all patients. Additional linear ablation was performed in 10 of 41 (24%) patients. The total radiofrequency duration was 64 ± 32 min. When AF could be terminated, the radio-frequency duration to obtain AF termination was 39 ± 22 min. The total procedure duration was 247 ± 89 min. The characteristics of patients with and without AF termination are shown in Table 3. Among baseline characteristics, failure to obtain AF termination was associated with higher LA LGE burden ($p < 0.001$), a higher number of re-entrant regions ($p < 0.001$), and longer AF duration ($p = 0.008$). LA LGE and re-entrant activity data in patients with and without AF termination are shown in Figure 5. At multivariable analysis, the number of re-entrant regions was independently related to successful AF termination ($R^2 = 0.42$, $p = 0.03$ when combined with LA LGE, $R^2 = 0.43$, $p = 0.03$ when combined with AF duration), whereas LA LGE and AF duration was not ($R^2 = 0.11$, $p = 0.09$ and $R^2 = 0.08$, $p = 0.17$, respectively). Among procedural characteristics, failure to obtain AF termination was associated with longer procedure time ($p <0.001$), prolonged RF duration ($p = 0.006$), and a higher rate of linear ablation ($p = 0.001$).

### FOLLOW-UP

Of the 41 patients, 6 were lost to follow-up, and 1 died at 6 months of a noncardiac cause. Therefore, follow-up was available in only 34 patients. Over a mean follow-up duration of 10.6 ± 2.4 months, 25 (74%) patients remained free of AF. Atrial tachycardia was detected in 7 (21%) patients. Patients remaining free of AF were younger (52 ± 11 years vs. 62 ± 10 years; $p = 0.04$), showed less prolonged uninterrupted AF duration (7.0 ± 5.7 months vs. 12.4 ± 6.1 months; $p = 0.03$), and had lower amounts of LA LGE (21 ± 5% vs. 27 ± 5% of the wall; $p = 0.02$). No significant difference was found in terms of sex, atrial volume, number of re-entrant regions on ECGI, or acute AF termination.

## DISCUSSION

This study demonstrates that in patients with persistent AF: 1) the amount of LGE is related to the number of regions exhibiting re-entry; 2) re-entrant activity clusters to LGE areas; and 3) the extent of LGE and re-entrant activity both affect procedural outcome during ablation.

### CORRELATES OF ATRIAL LGE AND RE-ENTRANT ACTIVITY

This study assessed re-entrant activity and atrial LGE in a series of 41 patients with persistent AF who were referred for catheter ablation. The population characteristics were similar to those of the usual population referred for persistent AF ablation in terms of age, sex, or AF duration (13). Atrial LGE was quantified using the method described by Oakes et al. (20), and the burden of LA LGE was in the range of prior reports in patients with persistent AF (23). Our results show that LA LGE relates to atrial volume and AF duration. This finding is consistent with past studies (20), and it supports the use of LGE CMR to

assess atrial remodeling. In the present study, LGE was also quantified on the right atrium. However, the relationships with clinical characteristics were weaker when considering the LGE burden on the right atrium and on both atria, a finding suggesting that CMR assessment of fibrosis is less robust on the right atrium than on the left atrium. However, this finding could also reflect a distinct mechanism of re-entry because of structural or functional differences between the left and right atria (28). ECGI was performed using a method described previously, and the mean number of re-entrant regions identified per patient was found to be similar (13). We observed a positive relationship between the number of re-entrant regions and both the LA volume and LGE burden, with LA LGE being the only independent predictor of re-entrant activity on multivariable analysis. This finding is consistent with prior experimental and modeling reports. Using optical mapping and computer modeling, Tanaka et al. (19) had demonstrated an impact of fibrosis on wave dynamics during AF in a sheep model of heart failure. In addition, the same group had reported a positive correlation between the number of phase singularities observed by optical mapping during fibrillation on 2-dimensional monolayers of cardiac cells and the amount of fibroblasts present in the preparation (17). Finally, a clinical study in patients with persistent AF had reported an inverse relationship between the extent of LGE on CMR and the AF cycle length as measured in the left appendage (29). Thus a growing body of evidence suggests that fibrosis burden is related to the global complexity of AF mechanisms. In the present study the relationship between the number of re-entrant regions and the burden of LA LGE was only fair ($R = 0.52$). This finding could be explained by the following: 1) the variability of the quantification of both re-entrant regions and LA LGE; 2) the role of right atrial LGE; and 3) the role of electrophysiological remodeling and triggers, which were not assessed in this study.

## RELATIONSHIP BETWEEN RE-ENTRANT ACTIVITY AND LOCAL LGE CHARACTERISTICS

In this study, regional analysis was performed only on a subset of patients because image noise is expected to affect local LGE characteristics and because with currently available methods, the high spatial resolution of LGE images is still associated with substantial noise. A subset of 20 patients was thus selected on the basis of optimal LGE CMR image quality. By showing different local LGE density values in re-entrant regions as compared with the remaining atrial tissue, our results showed that re-entrant activity clusters to a specific LGE pattern. We found a local LGE density of 0.35 on re-entrant regions (vs. <0.15 elsewhere), a finding indicating that these regions occur close to LGE. The spatial correlation between re-entrant activity and fibrosis in AF is still debated. In a recent study, Chrispin et al. (30) reported a lack of regional association between atrial LGE and rotors identified using the FIRM (Focal Impulse and Rotor Mapping) technology in 9 patients with persistent AF. However, a growing body of evidence supports the role of fibrosis in anchoring re-entry during AF. This includes prior experimental and modeling studies (17–19,31,32), as well as a prior clinical study reporting a clustering of complex fractionated atrial electrograms around fibrotic areas as assessed with CMR (29). Our results are also consistent with a recent computational study in which patient-specific models were built on CMR anatomic and LGE data in patients with persistent AF (33), thereby showing that simulated AF episodes are perpetuated by re-entrant drivers persisting in LGE boundary zones. This finding brings new insight into the mechanisms of sustaining re-entry at specific atrial

locations. It suggests that structural characteristics provide an anatomic substrate for re-entry. This may also explain how localized ablation of these sites results in AF organization or termination, as opposed to a purely functional phenomenon, in which ablation would displace re-entry. However, the spatial resolution of the techniques used in the current study does not allow a detailed analysis of the local substrate. Therefore, additional research is desirable to analyze further how re-entrant drivers anchor, and particularly to discriminate between structural and functional re-entry mechanisms. Although significant differences were found between LGE characteristics at re-entrant regions and in the rest of the atria, a substantial overlap persists, which makes it difficult to predict the location of re-entrant regions on the basis of CMR only (Figure 4). Although most re-entrant regions were observed in LGE areas, a substantial number of sites with LGE did not harbor re-entrant activity (LGE lacks specificity to predict reentry locations). This finding may reflect limitations of the proposed techniques to characterize fibrosis and re-entrant activity, as well as other confounding factors involved in arrhythmogenesis, such as patient-specific trigger activity and wave front directions, which were not characterized in this study (34,35). This particular issue could be addressed by computer modeling studies (36).

## PREDICTORS OF AF TERMINATION BY CATHETER ABLATION

This study used catheter ablation methods and endpoints described before, with a same rate of short-term procedural success (13). In this study, failure to achieve AF termination was not found to be significantly related to atrial volume. This observation contradicts the findings of other studies (37,38), and considering that the ablation targeting reentrant regions should not be responsible for this discrepancy, this result should be confirmed on a broader population. Failure to obtain AF termination was associated with AF duration, number of reentrant regions, and LA LGE. The relationship with AF duration and fibrosis is consistent with the findings of prior studies (13,23). The relationship with the number of re-entrant regions suggests that, beyond ablation targeting, the quantification of AF complexity by ECGI may be an interesting noninvasive tool to select ablation candidates. Indeed, in our study re-entrant activity was independently related to short-term procedural success on multivariable analysis, whereas atrial LGE and AF duration was not.

## STUDY LIMITATIONS

The first limitation of this study is related to the robustness of atrial fibrosis quantification. Atrial LGE mapping and quantification with CMR have been validated on the left atrium but not on the right atrium. However, we chose to segment LGE on both atria because ECGI results are computed using biatrial geometry. In addition, the current spatial resolution of CMR is still suboptimal, particularly in the slice thickness direction (2.5 mm). We acknowledge that this may have affected our results, especially in areas where the orientation of the wall is “in plane,” such as the atrial roof. Unfortunately, substrate mapping was not performed during the procedure; therefore, no voltage data were available to corroborate CMR findings (39).

The second limitation is related to the arbitrary choice of a threshold on phase singularity statistics to define a re-entrant region. Defining a threshold was necessary so that the atrial surface could be divided into regions of high and low levels of re-entrant activity. However,

experimental validation of such thresholding is lacking, and the reproducibility of reentrant region counting, which was used in this study as a surrogate for AF complexity, should be addressed by future studies. This validation would be critical before considering the use of ECGI to select patients undergoing catheter ablation. In addition, and for practical reasons, AF was not re-induced in the present study after ablation of a first set of re-entrant drivers. Similarly, we acknowledge that processing ECGI signals with phase mapping can lead to over-detection of re-entrant activities (40). The mode of AF induction was heterogeneous in the studied population (pacing induced in patients presenting in sinus rhythm, spontaneous in others). In patients presenting in sinus rhythm, ECGI was performed 30 min after AF induction to reach a steady state. However, the mode of induction and the duration of the ongoing AF episode may have affected our results. We chose not to exclude patients presenting in sinus rhythm, to cover the broad spectrum of persistent AF presentations. However, we agree that the small number of patients limits the strength of our conclusions.

One limitation of the proposed regional analysis is related to potential misregistration between CMR and ECGI geometries. Of note, the mean registration error of 3 mm reported here refers to a mean distance between CMR and ECGI meshes after registration and therefore to errors along the direction perpendicular to both surfaces. The accuracy of registration on the surface is expected to be of much lower amplitude, although there is no solution to quantify it in a clinical setting. To limit the impact of misregistration, local LGE descriptors were computed over quite large regions (5 mm). However, registration errors should lead to an underestimation rather than an overestimation of re-entry versus LGE relationships.

The ablation strategy was not limited to re-entrant drivers because pulmonary vein isolation and linear lesions could also be performed. In addition, ablation was targeted under fluoroscopic guidance in most of the patients because electroanatomic mapping systems were not routinely used. Therefore, procedural endpoint and follow-up data should be interpreted carefully, knowing that the ablation comprised both driver and nondriver targets and that the targeting of re-entrant regions may have been suboptimal. However, the objective of the present study was not to analyze the results of catheter ablation in persistent AF, but rather to describe the relationship between LGE and re-entrant activity in these patients at baseline.

## CONCLUSIONS

In patients with persistent AF, the number of regions with high re-entrant activity during AF assessed with ECGI relates to the amount of LGE on CMR. Re-entries cluster to LGE areas. The extent of LGE and re-entrant activity both impact procedural outcome during ablation.

## Supplementary Material

Refer to Web version on PubMed Central for supplementary material.

## Acknowledgments

The research leading to these results received funding from l'Agence Nationale de la Recherche (ANR) under Grant Agreements Equipex MUSIC ANR-11-EQPX-0030, TEMPO ANR-12-BSV1-029, and IHU LIRYC ANR-10-IAHU-04; from the European Union Seventh Framework Programme (FP7/2007-2013) under Grant Agreement HEALTH-F2-2010-261057; and from the National Institutes of Health (Pioneer Award DP1HL123271 to Dr. Trayanova). Drs. Haïssaguerre, Hocini, and Jaïs are stockowners in CardioInsight, Inc. Dr. Remi Dubois is a paid consultant for and has received royalties from CardioInsight, Inc. Dr. Jatin Relan is an employee of St. Jude Medical.

## ABBREVIATIONS AND ACRONYMS

| | |
|---|---|
| **AF** | atrial fibrillation |
| **CMR** | cardiac magnetic resonance |
| **ECGI** | electrocardiographic imaging |
| **LA** | left atrial |
| **LGE** | late gadolinium enhanced/enhancement |

## References

1. Kannel WB, Abbott RD, Savage DD, et al. Epidemiologic features of chronic atrial fibrillation: the Framingham study. N Engl J Med. 1982; 306:1018–22. [PubMed: 7062992]
2. Mandapati R, Skanes A, Chen J, et al. Stable microreentrant sources as a mechanism of atrial fibrillation in the isolated sheep heart. Circulation. 2000; 101:194–9. [PubMed: 10637208]
3. Jalife J, Berenfeld O, Mansour M. Mother rotors and fibrillatory conduction: a mechanism of atrial fibrillation. Cardiovasc Res. 2002; 54:204–16. [PubMed: 12062327]
4. Haïssaguerre M, Hocini M, Sanders P, et al. Localized sources maintaining atrial fibrillation organized by prior ablation. Circulation. 2006; 113:616–25. [PubMed: 16461833]
5. Ramanathan C, Ghanem RN, Jia P, et al. Noninvasive electrocardiographic imaging for cardiac electrophysiology and arrhythmia. Nat Med. 2004; 10:422–8. [PubMed: 15034569]
6. Oster HS, Taccardi B, Lux RL, et al. Noninvasive electrocardiographic imaging: reconstruction of epicardial potentials, electrograms, and isochrones and localization of single and multiple electrocardiac events. Circulation. 1997; 96:1012–24. [PubMed: 9264513]
7. Burnes JE, Taccardi B, Rudy Y. A noninvasive imaging modality for cardiac arrhythmias. Circulation. 2000; 102:2152–8. [PubMed: 11044435]
8. Wang Y, Cuculich PS, Zhang J, et al. Noninvasive electroanatomic mapping of human ventricular arrhythmias with electrocardiographic imaging. Sci Transl Med. 2011; 3:98ra84.
9. Haïssaguerre M, Hocini M, Shah AJ, et al. Noninvasive panoramic mapping of human atrial fibrillation mechanisms: a feasibility report. J Cardiovasc Electrophysiol. 2013; 24:711–7. [PubMed: 23373588]
10. Shah AJ, Hocini M, Xhaet O, et al. Validation of novel 3D electrocardiographic mapping of atrial tachycardias by invasive mapping and ablation: a multicenter study. J Am Coll Cardiol. 2013; 62:889–97. [PubMed: 23727090]
11. Ploux S, Lumens J, Whinnett Z, et al. Noninvasive electrocardiographic mapping to improve patient selection for cardiac resynchronization therapy: beyond QRS duration and left bundle branch block morphology. J Am Coll Cardiol. 2013; 61:2435–43. [PubMed: 23602768]
12. Narayan SM, Krummen DE, Shivkumar K, et al. Treatment of atrial fibrillation by the ablation of localized sources: CONFIRM (Conventional Ablation for Atrial Fibrillation With or Without Focal Impulse and Rotor Modulation) trial. J Am Coll Cardiol. 2012; 60:628–36. [PubMed: 22818076]
13. Haïssaguerre M, Hocini M, Denis A, et al. Driver domains in persistent atrial fibrillation. Circulation. 2014; 130:530–8. [PubMed: 25028391]

14. Kostin S, Klein G, Szalay Z, et al. Structural correlate of atrial fibrillation in human patients. Cardiovasc Res. 2002; 54:361–79. [PubMed: 12062341]
15. Platonov PG, Mitrofanova LB, Orshanskaya V, et al. Structural abnormalities in atrial walls are associated with presence and persistency of atrial fibrillation but not with age. J Am Coll Cardiol. 2011; 58:2225–32. [PubMed: 22078429]
16. Burstein B, Nattel S. Atrial fibrosis: mechanisms and clinical relevance in atrial fibrillation. J Am Coll Cardiol. 2008; 51:802–9. [PubMed: 18294563]
17. Zlochiver S, Muñoz V, Vikstrom KL, et al. Electrotonic myofibroblast-to-myocyte coupling increases propensity to reentrant arrhythmias in two-dimensional cardiac monolayers. Biophys J. 2008; 95:4469–80. [PubMed: 18658226]
18. Everett TH 4th, Wilson EE, Verheule S, et al. Structural atrial remodeling alters the substrate and spatiotemporal organization of atrial fibrillation: a comparison in canine models of structural and electrical atrial remodeling. Am J Physiol Heart Circ Physiol. 2006; 291:H2911–23. [PubMed: 16877548]
19. Tanaka K, Zlochiver S, Vikstrom KL, et al. Spatial distribution of fibrosis governs fibrillation wave dynamics in the posterior left atrium during heart failure. Circ Res. 2007; 101:839–47. [PubMed: 17704207]
20. Oakes RS, Badger TJ, Kholmovski EG, et al. Detection and quantification of left atrial structural remodeling using delayed enhancement MRI in patients with atrial fibrillation. Circulation. 2009; 119:1758–67. [PubMed: 19307477]
21. McGann C, Akoum N, Patel A, et al. Atrial fibrillation ablation outcome is predicted by left atrial remodeling on MRI. Circ Arrhythm Electrophysiol. 2014; 7:23–30. [PubMed: 24363354]
22. January CT, Wann LS, Alpert JS, et al. 2014 AHA/ACC/HRS guideline for the management of patients with atrial fibrillation: a report of the American College of Cardiology/American Heart Association Task Force on Practice Guidelines and the Heart Rhythm Society. Circulation. 2014; 130:e199–267. [PubMed: 24682347]
23. Marrouche NF, Wilber D, Hindricks G, et al. Association of atrial tissue fibrosis identified by delayed enhancement MRI and atrial fibrillation catheter ablation: the DECAAF study. JAMA. 2014; 311:498–506. [PubMed: 24496537]
24. Kim, EY., Johnson, H., Williams, N. [Accessed January 27, 2012] Affine transformation for landmark based registration initializer in ITK. MIDAS J [serial online]. 2011. Available at: http://hdl.handle.net/10380/3299
25. Horn BK. Closed-form solution of absolute orientation using unit quaternions. J Opt Soc Am. 1987; 4:629–42.
26. Shah AJ, Miyazaki S, Jadidi AS, et al. Ablation of persistent atrial fibrillation: AF termination is the end point. Card Electrophysiol Clin. 2012; 4:335–42. [PubMed: 26939953]
27. Vittinghoff E, McCulloch CE. Relaxing the rule of ten events per variable in logistic and Cox regression. Am J Epidemiol. 2007; 165:710–8. [PubMed: 17182981]
28. Li D, Zhang L, Kneller J, Nattel S. Potential ionic mechanism for repolarization differences between canine right and left atrium. Circ Res. 2001; 88:1168–75. [PubMed: 11397783]
29. Jadidi AS, Cochet H, Shah AJ, et al. Inverse relationship between fractionated electrograms and atrial fibrosis in persistent atrial fibrillation: combined magnetic resonance imaging and high-density mapping. J Am Coll Cardiol. 2013; 62:802–12. [PubMed: 23727084]
30. Chrispin J, Gucuk Ipek E, Zahid S, et al. Lack of regional association between atrial late gadolinium enhancement on cardiac magnetic resonance and atrial fibrillation rotors. Heart Rhythm. 2016; 13:654–60. [PubMed: 26569460]
31. Gonzales MJ, Vincent KP, Rappel WJ, et al. Structural contributions to fibrillatory rotors in a patient-derived computational model of the atria. Europace. 2014; 16(Suppl 4):iv3–10. [PubMed: 25362167]
32. Hansen BJ, Zhao J, Csepe TA, et al. Atrial fibrillation driven by micro-anatomic intramural re-entry revealed by simultaneous sub-epicardial and sub-endocardial optical mapping in explanted human hearts. Eur Heart J. 2015; 36:2390–401. [PubMed: 26059724]

33. Zahid S, Cochet H, Boyle PM, et al. Patient-derived models link re-entrant driver localization in atrial fibrillation to fibrosis spatial pattern. Cardiovasc Res. 2016; 110:443–54. [PubMed: 27056895]
34. Nattel S, Shiroshita-Takeshita A, Brundel BJ, et al. Mechanisms of atrial fibrillation: lessons from animal models. Prog Cardiovasc Dis. 2005; 48:9–28. [PubMed: 16194689]
35. Yamazaki M, Vaquero LM, Hou L, et al. Mechanisms of stretch-induced atrial fibrillation in the presence and the absence of adrenocholinergic stimulation: interplay between rotors and focal discharges. Heart Rhythm. 2009; 6:1009–17. [PubMed: 19560089]
36. McDowell KS, Vadakkumpadan F, Blake R, et al. Mechanistic inquiry into the role of tissue remodeling in fibrotic lesions in human atrial fibrillation. Biophys J. 2013; 104:2764–73. [PubMed: 23790385]
37. Berruezo A, Tamborero D, Mont L, et al. Pre-procedural predictors of atrial fibrillation recurrence after circumferential pulmonary vein ablation. Eur Heart J. 2007; 28:836–41. [PubMed: 17395676]
38. Abecasis J, Dourado R, Ferreira A, et al. Left atrial volume calculated by multi-detector computed tomography may predict successful pulmonary vein isolation in catheter ablation of atrial fibrillation. Europace. 2009; 11:1289–94. [PubMed: 19632980]
39. Kapa S, Desjardins B, Callans DJ, Marchlinski FE, Dixit S. Contact electroanatomic mapping derived voltage criteria for characterizing left atrial scar in patients undergoing ablation for atrial fibrillation. J Cardiovasc Electrophysiol. 2014; 25:1044–52. [PubMed: 24832482]
40. Vijayakumar R, Vasireddi SK, Cuculich PS, Faddis MN, Rudy Y. Methodology considerations in phase mapping of human cardiac arrhythmias. Circ Arrhythm Electrophysiol. 2016; 9:e004409. [PubMed: 27906655]

## APPENDIX

For supplemental text, references, and figures, please see the online version of this article.

## PERSPECTIVES

### COMPETENCY IN MEDICAL KNOWLEDGE 1

In patients with persistent atrial fibrillation, the number of regions with high re-entrant activity relates to the amount of atrial LGE on CMR.

### COMPETENCY IN MEDICAL KNOWLEDGE 2

Re-entrant activity responsible for sustaining AF clusters to LGE areas.

### TRANSLATIONAL OUTLOOK 1

Additional research is desirable to analyze further how re-entries anchor to specific atrial locations and particularly to discriminate between structural and functional re-entry mechanisms.

### TRANSLATIONAL OUTLOOK 2

Patient-specific assessment of structural remodeling and arrhythmia mechanisms during AF is feasible by combining CMR and ECGI data. This multimodal noninvasive approach may be of value to personalize biophysical models, with major potential applications for diagnosis, prognosis, and therapy.

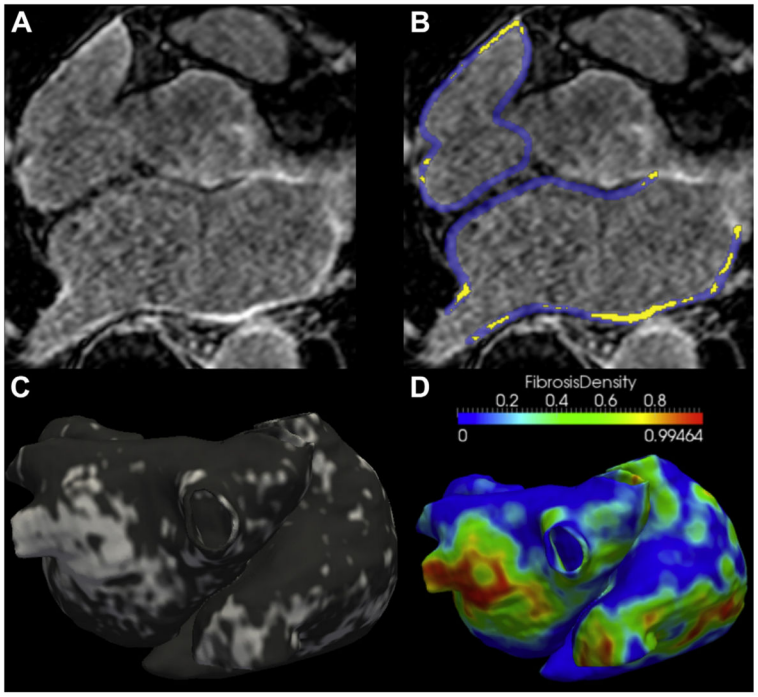


**FIGURE 1. Analysis of Atrial LGE on CMR**

A 61-year-old man with a history of persistent atrial fibrillation and no associated structural heart disease. On late gadolinium-enhanced (LGE) images, **(A)** areas of focal fibrosis are identified using manual segmentation of the atrial wall, and **(B)** adaptive thresholding on the histogram of myocardial voxels (**yellow** indicates late gadolinium enhancement). **(C)** The output of segmentation is a global quantification of late gadolinium enhancement expressed in a percentage of the wall and a map displaying late gadolinium-enhanced distribution over a biatrial surface (**white** indicates fibrosis). **(D)** A map of local late gadolinium-enhanced density (i.e., local burden of late gadolinium enhancement over a 5-mm neighborhood) is derived from late gadolinium-enhanced segmentation. CMR = cardiac magnetic resonance.

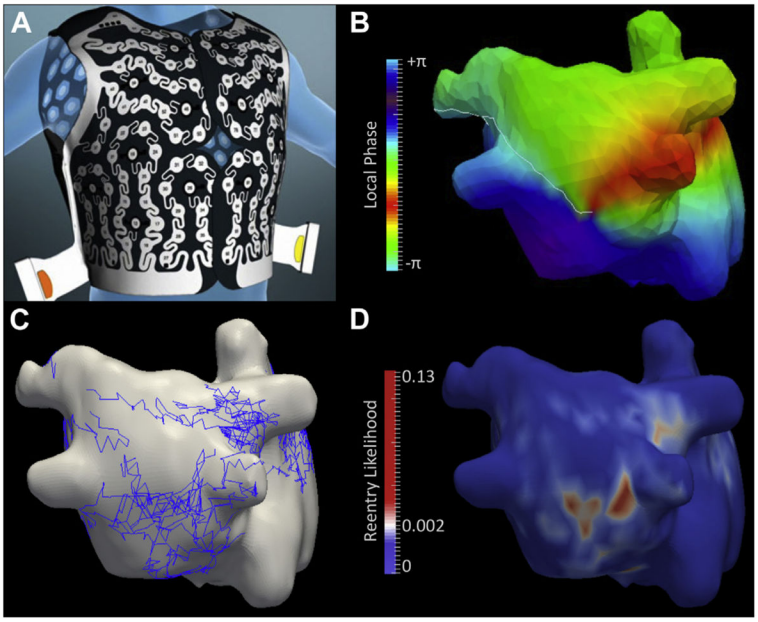


**FIGURE 2. Analysis of Re-Entrant Activity on ECGI**

A 54-year-old man with a history of persistent atrial fibrillation and no associated structural heart disease. **(A)** A multielectrode vest was placed on the patient's thorax, and the position of each electrode with respect to the atria was assessed using multidetector computed tomography. This geometric information was used to solve an inverse problem to reconstruct unipolar electrograms on the atrial surface from body surface potentials. **(B)** A phase mapping algorithm was applied on these unipolar electrograms to visualize activation during fibrillation and to identify re-entrant activity as phase singularities (color coding indicates local phase; **white line** indicates depolarization; a phase singularity can be seen on the posterior left atrial wall where all colors meet). **(C)** Automated tracking of phase singularities was implemented to collect their trajectories over the biatrial surface (trajectories in **blue**) throughout the whole mapping period (14 s in this example). **(D)** A cumulative map displaying the likelihood of re-entry was computed. On each point of the geometry, this refers to the probability of observing a re-entry at a given time frame. This map was used to define re-entrant regions to be targeted by ablation (**red** regions in **D**). ECGI = electrocardiographic imaging.

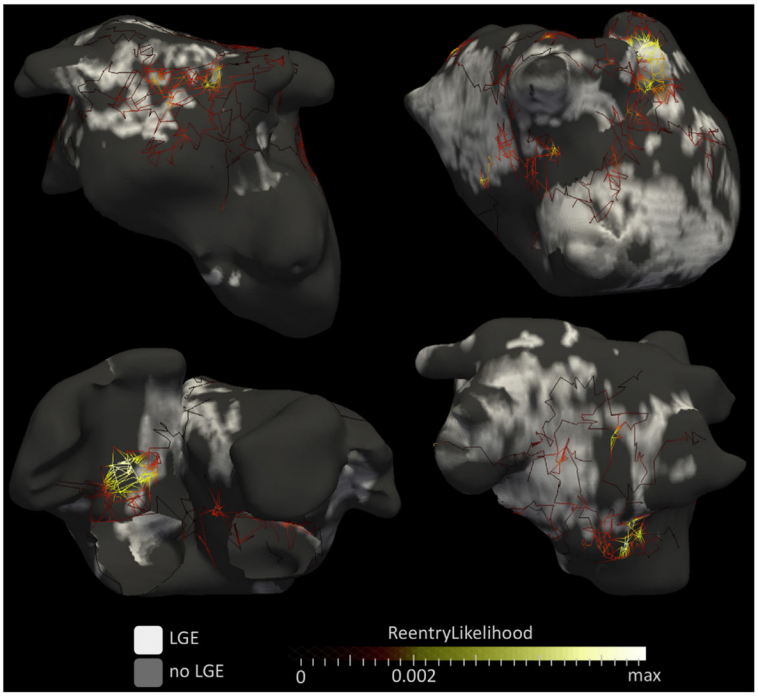


**FIGURE 3. Relationship Between Re-Entry Trajectories and Focal Fibrosis**

Results of cardiac magnetic resonance and electrocardiographic imaging are shown in 4 patients with a history of persistent AF and no structural heart disease (all men, age 54, 63, 57, and 48 years for **top left, top right, bottom left, and bottom right**, respectively). The trajectories of phase singularities, as defined in Figure 2, are overlaid on late gadolinium-enhanced (LGE) distribution (**white** indicates significant late gadolinium enhancement). Each trajectory is color coded according to the persistence of phase singularities at each point of the trajectory (i.e., the percentage of time a phase singularity was observed at each specific location). Therefore, **yellow** trajectories indicate sites of anchoring where a re-entrant activity meanders in a confined atrial location, whereas **dark red** trajectories indicate transit paths where re-entrant activity simply drifts. Visual analysis shows that anchoring sites (i.e., **yellow** trajectories) are located at the border of fibrotic areas, whereas trajectories observed either inside (e.g., **bottom right**) or outside (e.g., **upper left**) fibrotic areas appear as drifting sites (i.e., **straight dark red** trajectories).

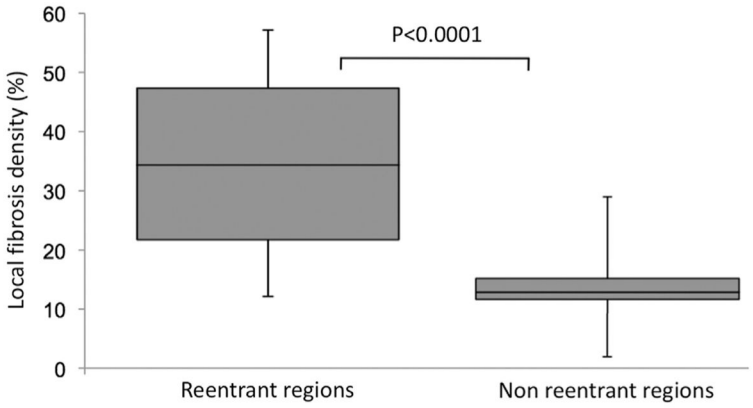


**FIGURE 4. Local LGE Density in Regions With Versus. Without Re-Entrant Activity (N = 20)**
LGE = late gadolinium enhancement.

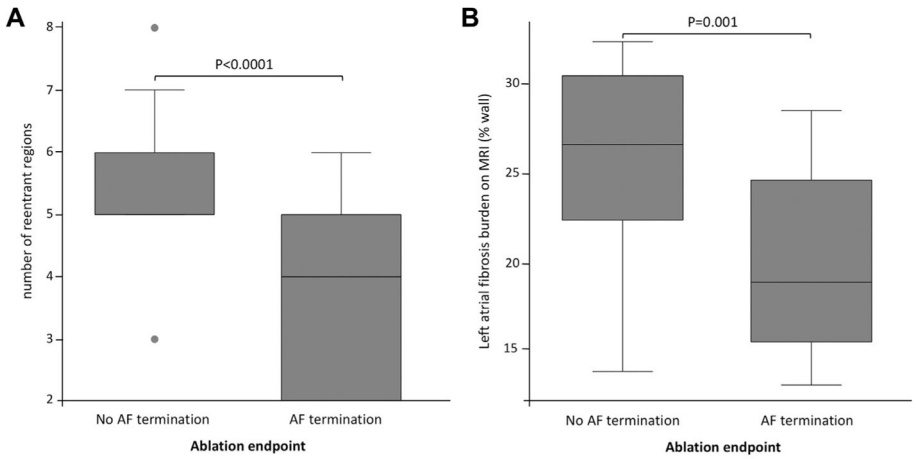


**FIGURE 5. Re-Entrant Activity and Left Atrial LGE in Patients With and Without Successful Termination of AF by Catheter Ablation (N = 41)**

AF = atrial fibrillation; LGE = late gadolinium enhancement; MRI = magnetic resonance imaging.

**TABLE 1**

Patient Characteristics

| | |
|---|---|
| Age (yrs) | 56 ± 12 |
| Male/female ratio | 35:6 |
| Uninterrupted AF duration (months) | 8.6 ± 6.5 |
| Associated structural heart disease | 5/41 (12%) |
| Rhythm at admission | |
| Sinus rhythm | 13/41 (32) |
| AF | 28/41 (68) |
| ECGI data | |
| Number of AF induced | 13/41 (32) |
| Number of re-entrant regions | 4 [3–6] |
| CMR data | |
| Left atrial volume (ml/m$^2$) | 74 ± 21 |
| Right atrial volume (ml/m$^2$) | 82 ± 28 |
| LGE burden on both atria (% of wall) | 19.9 ± 6.5 |
| LGE burden on both atria (ml) | 15.2 ± 6.4 |
| LGE burden on right atrium (% of wall) | 17.1 ± 7.9 |
| LGE burden on right atrium (ml) | 7.3 ± 5.4 |
| LGE burden on left atrium (% of wall) | 22.1 ± 5.9 |
| LGE burden on left atrium (ml) | 7.9 ± 3.2 |
| Procedural data | |
| Procedural duration (min) | 247 ± 89 |
| Total RF duration (min) | 64 ± 32 |
| RF duration until AF termination (min) * | 32 [23–58] |
| Re-entrant driver ablation | 41/41 (100) |
| Pulmonary vein isolation | 41/41 (100) |
| Linear ablation | 10/41 (24) |
| AF termination | 28/41 (68) |
| Termination into atrial tachycardia | 19/28 (68) |
| Termination into sinus rhythm | 9/28 (32) |

Continuous variables are expressed as mean± SD when of normal distribution and median [interquartile range: Q1 to Q3] otherwise. Categorical variables are expressed as fractions (%).

* RF duration until AF termination refers to the 28 of 41 patients who could have termination of AF.

AF = atrial fibrillation; CMR = cardiac magnetic resonance; ECGI = electrocardiographic imaging; LGE = late gadolinium-enhanced; RF = radiofrequency.

## TABLE 2

Correlates of Re-Entrant Activity

| **Univariable Analysis** | **R** | **p Value** |
|---|---|---|
| Age (yrs) | −0.05 | 0.78 |
| Female | 0.16 | 0.34 |
| Uninterrupted AF duration (months) | 0.45 | 0.005 |
| Associated structural heart disease | 0.06 | 0.75 |
| Left atrial volume (ml/$m^2$) | 0.35 | 0.04 |
| Right atrial volume (ml/$m^2$) | 0.25 | 0.16 |
| LGE burden on both atria (% of wall) | 0.38 | 0.03 |
| LGE burden on both atria (ml) | 0.25 | 0.17 |
| LGE burden on right atrium (% of wall) | 0.21 | 0.22 |
| LGE burden on right atrium (ml) | 0.05 | 0.75 |
| LGE burden on left atrium (% of wall) | 0.52 | 0.001 |
| LGE burden on left atrium (ml) | 0.44 | 0.006 |
| **Multivariable Analysis** | **$R^2$ Change** | |
| LGE burden on left atrium (% of wall) | 0.32 | 0.006 |
| Uninterrupted AF duration (months) | 0.03 | 0.27 |
| Left atrial volume (ml/$m^2$) | 0.0001 | 0.94 |

Abbreviations as in Table 1.

## TABLE 3

Predictors of AF Termination by Catheter Ablation at Univariable Analysis

| | AF Termination (N = 28) | No AF Termination (N = 13) | p Value |
|---|---|---|---|
| Age (yrs) | 58 ± 11 | 51 ± 13 | 0.10 |
| Male/female ratio | 24:4 | 11:2 | 0.93 |
| Uninterrupted AF duration (months) | 6.9 ± 4.7 | 12.5 ± 8.1 | 0.008 |
| Associated structural heart disease | 4/28 (14%) | 1/13 (8%) | 0.56 |
| ECGI data | | | |
| Number of re-entrant regions | 4 [2–5] | 6 [5–6] | <0.001 |
| CMR data | | | |
| Left atrial volume (ml/m$^2$) | 70 ± 22 | 81 ± 20 | 0.19 |
| Right atrial volume (ml/m$^2$) | 78 ± 27 | 86 ± 28 | 0.37 |
| LGE burden on both atria (% of wall) * | 18.5 ± 6.3 | 22.7 ± 6.9 | 0.02 |
| LGE burden on both atria (ml) * | 14.2 ± 6.6 | 17.4 ± 6.0 | 0.14 |
| LGE burden on right atrium (% of wall) * | 16.5 ± 7.7 | 18.1 ± 8.1 | 0.12 |
| LGE burden on right atrium (ml) * | 7.3 ± 6.1 | 7.4 ± 3.5 | 0.97 |
| LGE burden on left atrium (% of wall) * | 20.1 ± 5.1 | 26.2 ± 5.4 | <0.001 |
| LGE burden on left atrium (ml) * | 6.9 ± 2.4 | 10.0 ± 3.6 | 0.002 |
| Procedural data | | | |
| Procedural duration (min) | 217 ± 71 | 325 ± 87 | <0.001 |
| Total RF duration (min) | 53 ± 25 | 90 ± 34 | <0.001 |
| RF duration until AF termination (min) | 31 [21–49] | NA | NA |
| Linear ablation | 2/28 (7%) | 8/13 (62%) | 0.001 |

Continuous variables are expressed as mean± SD when of normal distribution and median [interquartile range: Q1 to Q3] otherwise. Categorical variables are expressed as fractions (%).

* The relationship between LGE burden and AF termination was assessed in the 37 of 41 patients eligible for LGE quantification.

NA = not applicable; other abbreviations as in Table 1.